# Functional Materials from Self-Assembled Bis-urea Macrocycles

Linda S. Shimizu,* Sahan R. Salpage, and Arthur A. Korous

Department of Chemistry and Biochemistry, University of South Carolina, Columbia, South Carolina 29208, United States

CONSPECTUS: This Account highlights the work from our laboratories on bis-urea macrocycles constructed from two C-shaped spacers and two urea groups. These simple molecular units assembled with high fidelity into columnar structures guided by the three-centered urea hydrogen bonding motif and aryl stacking interactions. Individual columns are aligned and closely packed together to afford functional and homogeneous microporous crystals. This approach allows for precise and rational control over the dimensions of the columnar structure simply by changing the small molecular unit. When the macrocyclic unit lacks a cavity, columnar assembly gives strong pillars. Strong pillars with external functional groups such as basic lone pairs can expand like clays to accept guests between the pillars. Macrocycles that contain sizable interior cavities assemble into porous molecular crystals with aligned, well-defined columnar pores that are accessible to gases and guests. Herein, we examine the optimal design of the macrocyclic unit

that leads to columnar assembly in high fidelity and probe the feasibility of incorporating a second functional group within the macrocycles.

The porous molecular crystals prepared through the self-assembly of bis-urea macrocycles display surface areas similar to zeolites but lower than MOFs. Their simple one-dimensional channels are well-suited for studying binding, investigating transport, diffusion and exchange, and monitoring the effects of encapsulation on reaction mechanism and product distribution. Guests that complement the size, shape, and polarity of the channels can be absorbed into these porous crystals with repeatable stoichiometry to form solid host−guest complexes. Heating or extraction with an organic solvent enables desorption or removal of the guest and subsequent recovery of the solid host. Further, these porous crystals can be used as containers for the selective [2 + 2] cycloadditions of small enones such as 2-cyclohexenone or 3-methyl-cyclopentenone, while larger hosts bind and facilitate the photodimerization of coumarin. When the host framework incorporates benzophenone, a triplet sensitizer, UV-irradiation in the presence of oxygen efficiently generates singlet oxygen. Complexes of this host were employed to influence the selectivity of photooxidations of 2-methyl-2-butene and cumene with singlet oxygen. Small systematic changes in the channel and bound reactants should enable systematic evaluation of the effects of channel dimensions, guest dimensions, and channel−guest interactions on the processes of absorption, diffusion, and reaction of guests within these nanochannels. Such studies could help in the development of new materials for separations, gas storage, and catalysis.
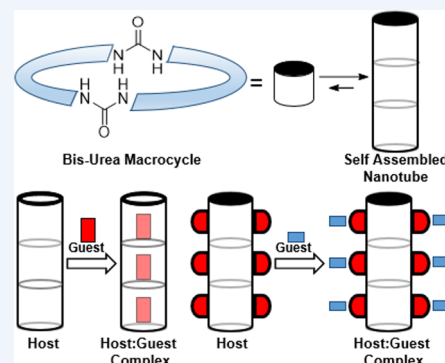
■ INTRODUCTION

Porous materials have demonstrated utility as sorbents,[1] separation supports,[2] and reaction templates[3] and are applicable to nanofluidics,[4] to catalysis,[5] and for storage of reactive materials such as gases and reagents.[6] Thus, it is not surprising that many different types of natural and synthetic porous materials have been identified or designed such as zeolites,[7] clays,[8] mesoporous silicates,[9,10] porous molecular crystals,[11] and metal−organic frameworks (MOF's).[12] This list is far from complete and merely serves to highlight the diversity of these materials. Indeed, the challenge lies not in identifying new porous materials but in designing the next generation of advanced functional materials to solve problems, answer questions, and probe processes.

The use of self-assembling systems to build functional materials through labile noncovalent interactions allows complex structures to be assembled from readily synthesizable small molecules and endows the system with dynamic attributes that could correct errors, repair damage (self-healing), and potentially make these materials responsive to external

stimuli.[13] The conceptually simple motif of self-assembling disks into columns or channels has proven to be widely applicable. Examples of self-assembling macrocycles include cyclic peptides,[14,15] carbazole arylene ethynylene macrocycles,[16] platinum ligated rings (Pt$_4$ rings),[17] and aromatic oligoamide macrocycles.[18] Over the past decade, our group has focused on developing a simple bis-urea macrocyclic unit that assembles into columnar structures with high fidelity and affords crystalline materials. These systems can be thought of as a subset of nanoporous molecular crystals, in which small molecular units are held together by only noncovalent interactions.[19] Our macrocycles are modularly constructed from two rigid C-shaped spacers and two urea groups. Depending on the size of the macrocycle's interior cavity, these simple building blocks assemble to give either strong pillars or columns with homogeneous channels. For example,
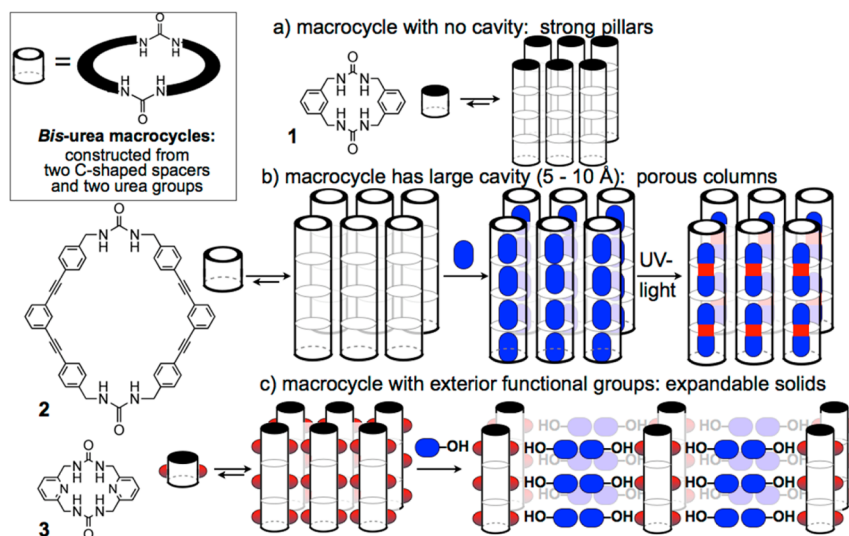
Figure 1. The bis-urea macrocycle assembly motif. (a) Macrocycles that lack pores assemble into robust one-dimensional pillars.[20] (b) Macrocycles that contain sizable cavities give homogeneous channels that can bind guests, can facilitate selective reactions, and can be used to study molecular transport.[21] (c) Macrocycles with exterior groups (red) may expand to absorb guests that contain complementary functional groups. Columns of **3** contain exterior hydrogen bond acceptors that drive the absorption of alcohol guests.[23]
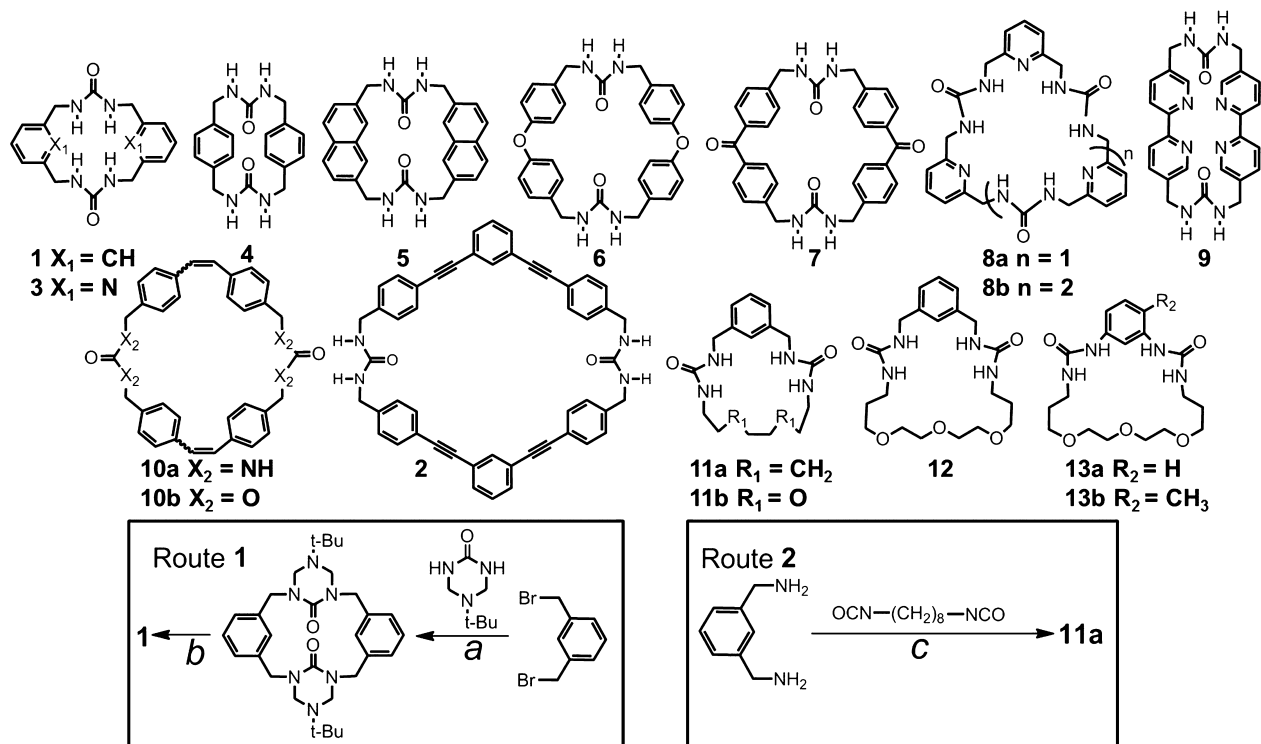

Figure 2. Bis-urea macrocycles are constructed by the modular synthesis of ureas and C-shaped spacers to afford macrocycles with different sizes, shapes, and functionalities. Two general strategies have been used. Reagents and conditions: (*a*) NaH, THF, reflux; (*b*) 20% aq. diethanol amine pH ≈ 2−3, MeOH, reflux; (*c*) diisocyanate and diamine in CH_2Cl_2 or DMF.

the small *meta*-xylene derivative in Figure 1a has no internal cavity because the central aryl hydrogen atoms are nearly within van der Waals contact.[20] It self-assembles through urea hydrogen bonds to afford strong pillars. Larger macrocycles, such as the phenylethynylene derivative in Figure 1b, have an internal cavity, which upon columnar assembly affords homogeneous one-dimensional channels, whose dimensions are controlled by the size and shape of the macrocycle.[21] Single

columns pack together to give porous molecular crystals with aligned channels. Simple one-dimensional channels offer advantages over complex networked materials for detailed study of the processes of adsorption, diffusion, and reactions that may occur within their regular tubular topology. Diffusion of guests into microcavities and channels is a complex phenomenon that is of interest to biologists studying transport in cells, chemists investigating catalytic reactions and
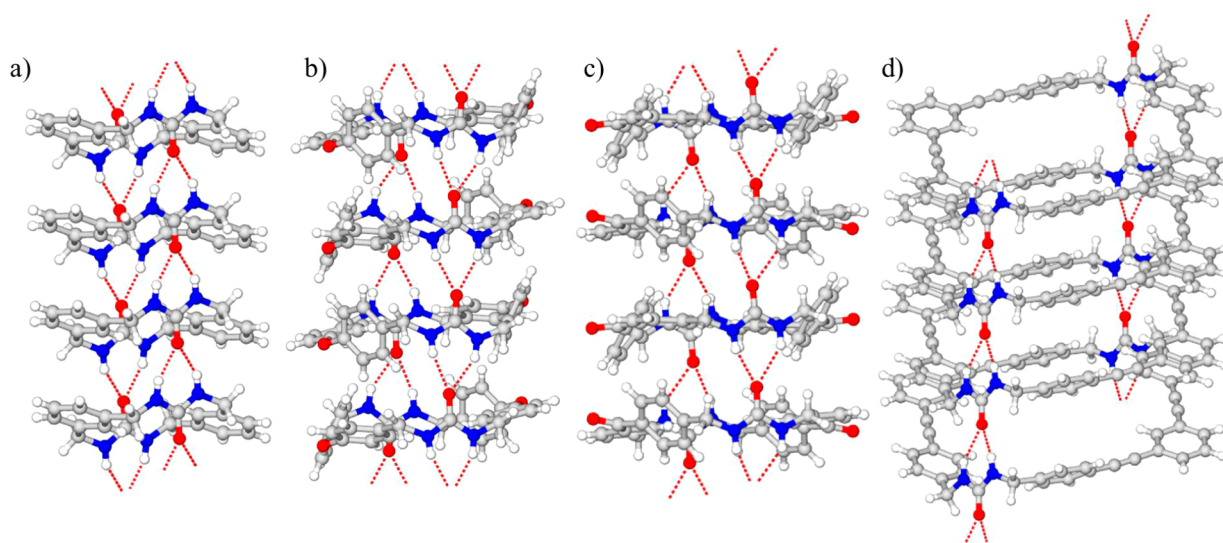
Figure 3. Views along a single column from the respective crystal structures of assembled bis-ureas show that the macrocycles are relatively planar with the urea groups oriented approximately perpendicular to the plane: (a) *m*-xylene **1**,[20] (b) phenylether **6** (acetic acid solvent removed for clarity),[31] (c) benzophenone **7** (DMSO solvent removed for clarity),[32] and (d) phenylethynylene **2** (nitrobenzene guests removed for clarity).[21]

separations, and theoreticians investigating geometrically constrained Brownian dynamics.[22]

Our approach can potentially organize and control the spatial arrangement of guests on both the interior and exterior of the columns. For example, a basic group on the exterior of the macrocycle (Figure 1c) can be used to drive the absorption of alcohol guests through hydrogen bond formation.[23] The distance between the individual strong pillars of the bis-urea assemblies can expand and contract like clays and absorb guests that are able to form interactions with the exterior functional group. This strategy provides a complementary method for organizing guests and is amenable to guests that would be excluded from internal channels due to their size or shape. This Account focuses on our efforts to (1) understand the scope and limits of this assembly motif, (2) investigate the feasibility of including functional groups on the interior or exterior of the macrocycle, (3) examine the relationship of column size and shape to the uptake and organization of guests, and finally (4) investigate the use of these porous hosts as containers to facilitate photocycloadditions and photooxidations.

■ DESIGN

Ureas are a well-studied assembly motif in supramolecular chemistry. The urea NH groups are good hydrogen bond donors, and the urea oxygen is an excellent acceptor as reflected by their α and β values (α = 3.0, β = 8.2).[24] Early crystallographic work led to a set of empirical guidelines for predicting the assembly patterns of ureas.[25] Since that time, urea building units have been used to make columns, fibers, sheets, tapes, capsules, and gels.[26,27] Our work has focused on incorporating ureas into a simple assembly unit, a macrocyclic bis-urea, which is constructed from two C-shaped spacers and two urea groups. The spacers should be rigid, incorporate a bend angle (C-shape), not introduce strain, and afford a relatively planar macrocycle conformation. Most importantly, the spacer should help to preorganize the urea groups to facilitate columnar self-assembly. In addition, the rigid spacers serve to maintain open cavities of precise and predictable size. In general, two routes have been used to synthesize these macrocycles: (1) a protected urea is cyclized with benzyl

dibromides under basic conditions or (2) diisocyanates are reacted with corresponding diamines. Both strategies must be run in dilute conditions to favor macrocyclization over polymerization; however, the first route is advantageous because it affords a soluble protected bis-urea macrocycle that aids in isolation and purification. The protecting groups are removed with diethanolamine under acidic conditions.[20,28] Route 1 was used to construct macrocycles **1−10** from commercial or readily made precursors in 2−4 steps (Figure 2). Macrocycles **11−13** were obtained via direct condensation of the diisocyanates and diamines (route 2).[29] The bis-urea macrocycles in Figure 2 survey a range of cavity sizes from no interior cavities (**1**, **3**) to small cavities of 3−6 Å (**4−10**) to a large cavity of ~9 Å (**2**). These macrocycles also test the design parameters by probing the influence of flexibility (**11−13**) and interior functionality such as ethers (**11b−13**), carbonyls (**7**), pyridines (**3**, **8**), and bipyridines (**9**) on the assembly.

Columnar Assembly by Crystallization

Single crystals and microcrystals of bis-urea macrocycles were obtained by dissolving the macrocycle (10 mg in 2 mL of hot glacial acetic acid, DMSO, or DMF) followed by hot filtration and slow cooling, by vapor diffusion of MeOH, H_2O, or hexanes into solutions of the macrocycle (10 mg in 2 mL of DMSO) or from water under hydrothermal conditions. Though large single crystals are rare, microcrystals (~250 μm × 3 μm) are abundant and appear as long thin needles, which grow quickly along the direction of urea assembly.[30] PXRD of the bulk crystals and microcrystalline powders indicate that they are single phase and similar in structure to the single crystals.[21,30] Columnar assembly of these macrocyclic units is favored with high fidelity when the macrocycle is relatively planar with the urea groups oriented approximately perpendicular to the plane of the macrocycle. In each case, the columns are not empty but filled with solvent. For now, we will focus only on the urea assembly and will address the issue of encapsulated solvent later. Figure 3 illustrates the columnar assembly of four bis-urea macrocycles that conform to these design parameters. In each case, the macrocycles are held together by urea hydrogen bonds with distances that range from 2.85 to 3.05 Å and additional
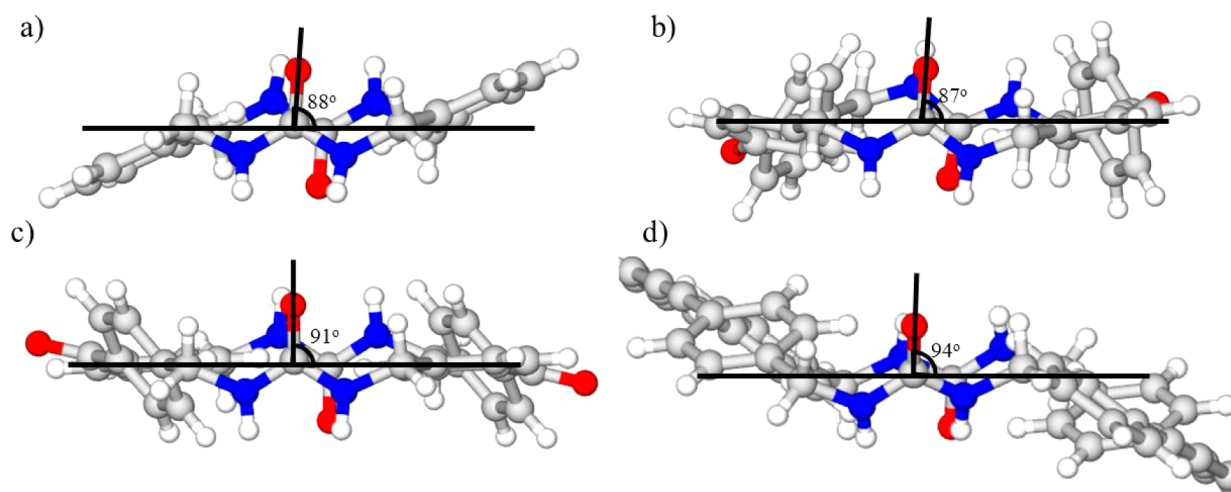
Figure 4. Further analysis from the crystal structures in Figure 3 illustrates the orientation of the urea groups with respect to the mean plane of the macrocycles as defined by the coordinates of ring atoms from the cif file using plane plugin in Mercury:[33] (a) *meta*-xylene **1** urea groups aligned at 88° with respect to the plane of the macrocycle; (b) phenylether **6** orients urea groups at 87°; (c) benzophenone **7** orients the urea groups at 91°; (d) phenylethynylene **2** orients the urea groups at 94°.
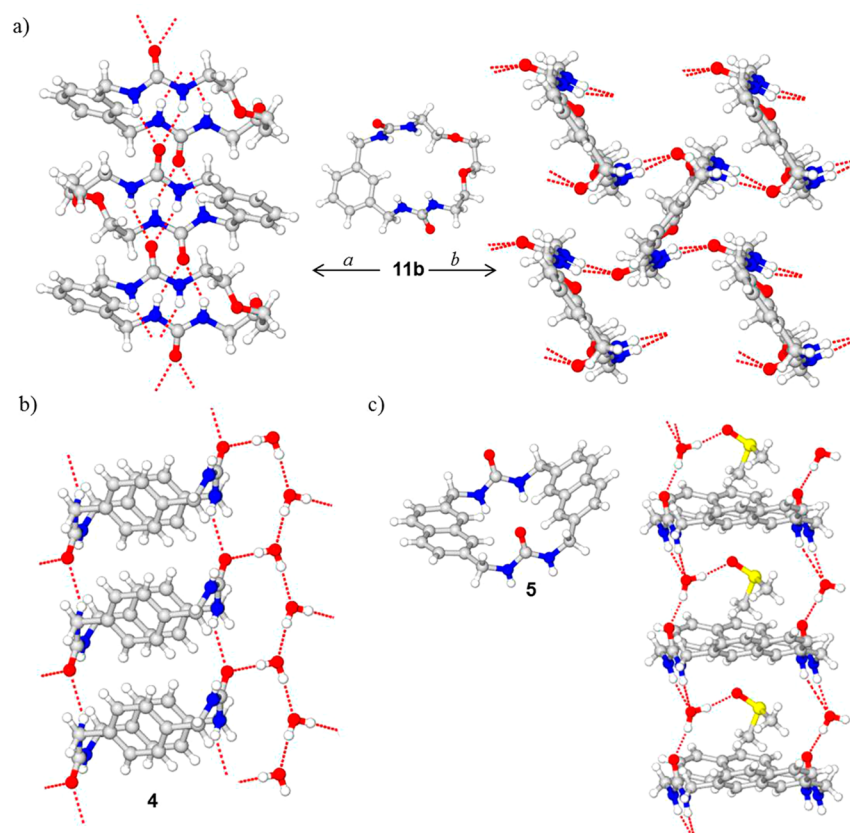

Figure 5. Macrocycles that deviate from key design parameters show lower fidelity for columnar assembly. (a) The greater flexibility of macrocycle **11b** leads to multiple crystal forms.[29] Conditions: (*a*) slow cool from AcOH; (*b*) slow evaporation of a 10:1 CH_2Cl_2/MeOH. (b) Strained *para*-xylene derivative **4** shows an altered assembly motif with intervening water molecules when crystallized in slow cooling DMSO.[38] (c) The bowl shape of **5** hinders the urea assembly motif. The macrocycle assembles via intervening water molecules.[39]

aryl stacking interactions or, in the case of **2**, interactions between the ethynes and aryl groups.[20,21,31,32] These interactions set repeat distances from 4.6 to 4.7 Å. In each of these structures, the urea group is nearly perpendicular with respect to the plane of the macrocycle. For example, *meta*-xylene **1** orients the urea group at ~88° with respect to the plane (Figure 4a). Similarly, phenylether **6**,[31] benzophenone **7**,[32] and phenylethynylene **2**[21] orient the urea groups at 87°, 91°, and 94° respectively (Figure 4b,c,d). In each structure, the urea groups within a single macrocycle are oppositely aligned, presumably to minimize dipole interactions.
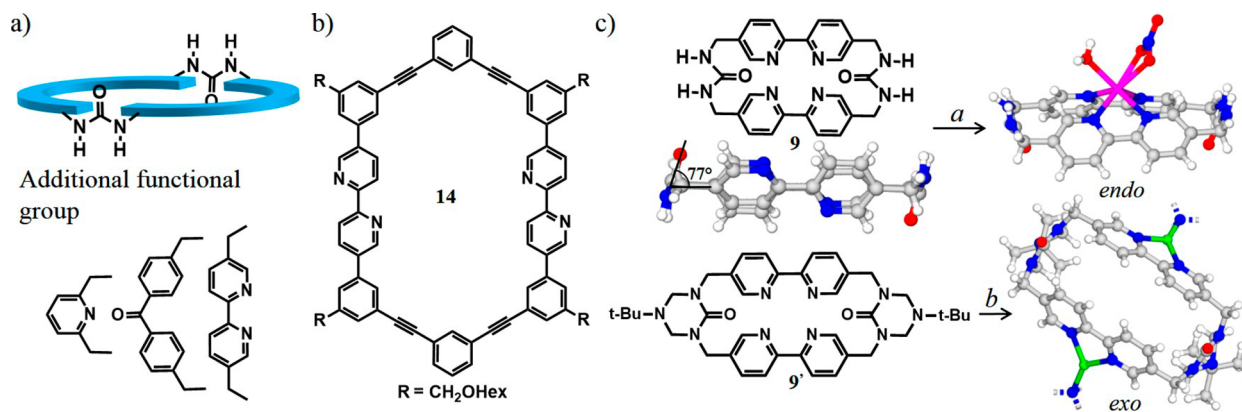
Figure 6. Macrocycles with multiple functional groups. (a) Schematic bis-urea macrocycles with C-spacers that have sensitizers, basic groups, or metal chelating groups. (b) The bipyridines in phenylacetylene **14** from Schlüter's group can rotate to form an interior "*endo*" or exterior "*exo*" binding modes.[41] (c) Bis-urea macrocycle **9** can also rotate to give *exo* or *endo* binding modes. The parent macrocycle **9** crystallized in a twisted *anti*-conformation with the ureas tilted 77° with respect to the plane. (*a*) The *endo* mode was observed in [Cd(**9**)(H$_2$O)(NO$_3$)$_2$].[40] (*b*) The *exo* mode was observed with the triazinanone protected **9′** {[Ag$_2$(**9′**)](SO$_3$CF$_3$)$_2$·unknown solvate}.[40]

The urea self-association is not the only interaction that can be used to guide column formation. Indeed, changing the urea NHs in **10a** for oxygens gives a stilbene dicarbonate macrocycle **10b**, which also showed columnar through short C−H⋯O hydrogen bonds and aryl stacking interactions.[34] These appeared to be less robust than the urea interactions and removal of guests caused loss of crystallinity. However, carbonate macrocycles are intriguing monomers for ring-opening polymerizations to afford polycarbonates, which may be of interest due to their processability and degradability.[35]

We surveyed a range of structures to test these design parameters and found that structures that are more flexible, have a different orientation of the urea groups, or are bowl shaped afford multiple crystal forms that depend on crystallization conditions. Macrocycles **11–13** incorporate a relatively flexible alkyl or ethylene glycol chain to study the effects of ring size and conformational mobility on assembly.[29] Similarly, tris (**8a**) and tetrapyridyl urea macrocycles (**8b**), which bind alkali metal cations[36] and form helical coordination polymers,[37] have additional methylene groups that increase their conformational mobility. In general, these changes reduced the fidelity of the columnar assembly motif and increased their solubility. Figure 5a illustrates how the more flexible macrocycle **11b** assembles into either columns or 2D herringbone structures depending upon the crystallization conditions. A closer examination of the columnar structures reveals that it is stabilized by both aryl stacking interactions and three centered urea interactions with the ureas oppositely aligned but tilted 34° from perpendicular. The interdigitated structure is also stabilized by the typical three centered urea motif; however, the ureas are aligned in parallel, and one urea group tilted 42° from perpendicular. There appears to be no stabilizing aryl stacking interactions. Computational studies suggested that the macrocycle has a number of low energy conformations and those with the parallel and antiparallel ureas are very close in energy. This flexibility likely accounts for the loss of control over assembly.

The *para*-xylene spacer appears to induce strain within its corresponding macrocycle **4**,[38] which reduces the macrocyclization efficiency and affects the subsequent assembled structure (Figure 5b). In this structure, one of the urea NH groups is twisted out of the plane to form a hydrogen bonding interaction with intervening water molecules. This leaves

columns stabilized by amide-type hydrogen bonding interactions. Figure 5c illustrates the steric problem posed by bowl shapes. Crystallization of naphthalene **5** under several conditions afforded similar molecular conformations but several types of assemblies. The bowl shaped naphthalenes arranged the ureas in parallel, a unit that assembled into extended columns (1 mg mL^{-1} in DMSO/H$_2$O, Figure 5c) or into lamellar structures (1 mg mL^{-1} in MeOH/H$_2$O).[39] The columns have interpenetrating water molecules and DMSO molecules that form hydrogen bonds with the ureas in lieu of the urea self-association. These examples illustrated how the information needed to specify columnar assembly has been lost and reinforced the importance of the original design parameters.

Multifunctional Macrocycles

It is a challenge to append a second set of units on an assembly system to impart further function. The units used to impart an additional function, such as binding interactions or catalysis, must be orthogonal in both their role and orientation to those that direct supramolecular assembly. In our small building unit, ureas guide the assembly through relatively weak hydrogen bonds, and any appended groups are poised in close proximity to the ureas. If the new functional group contains lone pairs, it could compete with the urea oxygen as a hydrogen bond acceptor and potentially disrupt the assembly. We began by altering the C-shaped spacer to include a sensitizer (benzophenone) or basic groups (pyridine or bipyridines) within the macrocycle. Benzophenone spacers present aryl ketones, and their incorporation in host **7** did not alter the columnar assembly (Figure 3b). Macrocycle **9** combines ureas and bipyridines through the bipyridine's conformationally mobile 5,5′ positions (Figure 6). This allows the bipyridines to freely rotate, an action that can exchange an interior (*endo*) metal binding site for an exterior (*exo*) site.[40] Macrocycle **14** from Schlüter's group can rotate to access both *exo* and *endo* binding sites and reacts with 2 equiv of [Ru(bipy)$_2$Cl$_2$] to afford the homo dinuclear *exo* coordinated macrocycle.[41] In free host **9**, the bipyridines adopted an *anti*-coplanar configuration and the urea groups are tilted 77° with respect to the plane of the macrocycle (Figure 6c). As expected, host **9** readily interacts with transition metals, but the affinity differs from the expected Irvings−Williams order,[42] experimentally
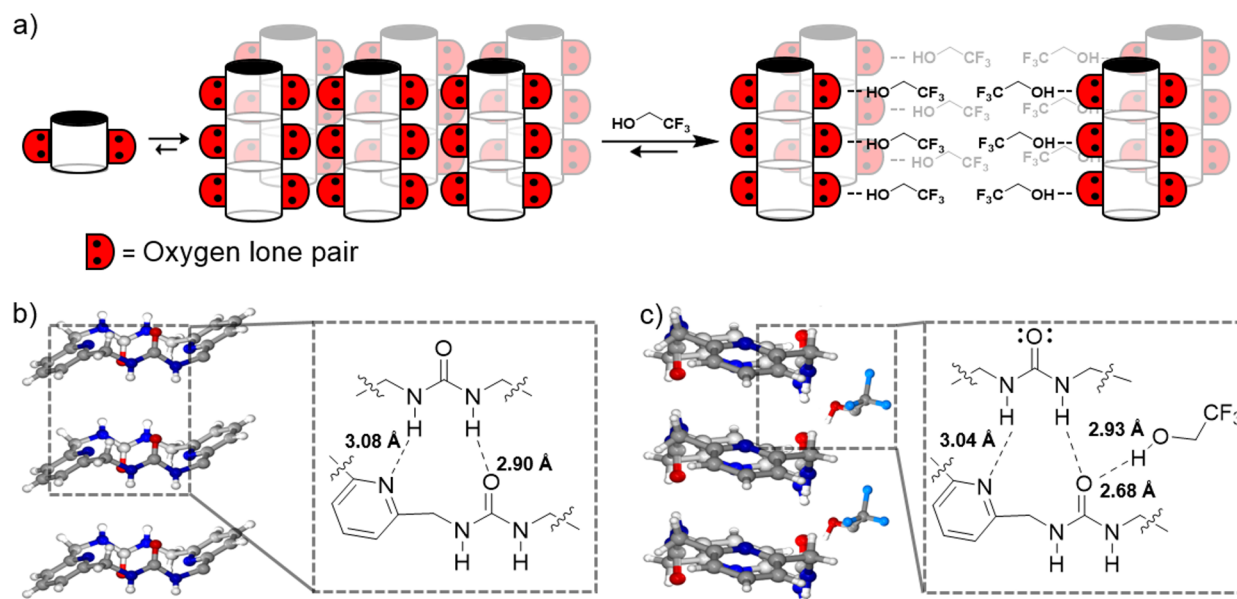
Figure 7. Pyridine bis-urea macrocycle **3** assembles into nanotubes through a robust but altered hydrogen bonding motif that has the urea NH's forming hydrogen bonds with two different acceptors.[23] (a) Schematic depiction of the nanotubes. The exterior of each nanotube has oxygen lone pairs that can participate in hydrogen bonding with guests. (b) Host **3** crystallized from DMSO/MeOH gives columns organized via two hydrogen bonds between the urea NH and the neighboring urea oxygen with an N(H)···O distance of 2.904 Å and the urea NH and pyridine with NH···N distance of 3.082 Å. (c) Host **3** crystallized from DMSO/TFE gives similar hydrogen bonded columns that are separated by TFE layers that for hydrogen bonds to the urea oxygen with OH···O distance of 2.683 Å.

suggesting that some of the metal cations interact with the constrained *endo*-conformer. An *endo* complex, $[Cd(9)(H_2O)\text{-}(NO_3)_2]$, was prepared by slow evaporation of a solution of $Cd(NO_3)_2$ and **9** from THF (10^{-5} M, 1:1 molar ratio).[40] The bipyridines are rotated inward coordinating to a single Cd^{2+} ion (Figure 6c), which also has water and nitrate in its coordination sphere. The nitrate also interacts with one of the urea NH groups, suggesting that we need to use metal salts with less basic counterions to favor the typical urea assembly. An *exo* complex with silver $\{[Ag_2(9')](SO_3CF_3)_2 \cdot \text{unknown solvate}\}$ was prepared from the urea protected derivative of **9'** (Figure 6c). Each bipyridine group is rotated outward to bind with two Ag^+ ions. We are investigating complexes of **9** with silver[43] due to Ag(I)'s catalytic properties,[44] as well as complexes with Ru(II), Ir(II), and Pt(II) as such complexes may have applications in catalysis[45] and for sensor materials.[46]

Literature predicts that the pyridine nitrogen ($\beta = 7.2$) should be a slightly weaker hydrogen bond acceptor than the urea oxygen ($\beta = 8.2$).[24] These values are based on flexible open chain systems, while **3** places the pyridine and urea groups in close proximity within a small macrocycle, which lacks an interior cavity. Geometry and proximity are known to influence the strength of donors and acceptors.[47] Vapor diffusion of MeOH into a solution of **3** (10 mg in 2 mL of DMSO) gave X-ray quality single crystals that displayed close packed columns.[23] A view along a single column reveals that the individual macrocycles are held together by an altered hydrogen bonding motif in which the urea NH's interact with two different acceptors (Figure 7). The shorter hydrogen bond is formed with the urea carbonyl oxygen (N−O distance of 2.904 Å) versus with the pyridine nitrogen (N−N distance of 3.082 Å). Given that crystal form has no interior channels or obvious pores, we were surprised to observe a type 1 gas adsorption isotherm with both hydrogen and carbon dioxide. A second crystal form **3**·TFE, which suggested a plausible explanation of

the gas adsorption data, was obtained by the vapor diffusion of TFE into a solution of **3** (10 mg in 2 mL of DMSO) and showed identical columnar assembly. However, here TFE is interpenetrated between the columnar layers through hydrogen bonding interactions with the formerly unsatisfied lone pair that resides on the exterior of the pillars. The TFE forms hydrogen bonds to the urea oxygen with an OH···O distance of 2.683(7) Å. Perhaps the gases (H_2 and CO_2) are also accommodated between strong pillars of assembled **3**.

These two crystal forms were readily interconverted. Simply heating **3**·TFE induced desorption of TFE and afforded closely packed columns of **3**.[23] Microcrystals and powders of assembled **3** that were exposed to vapors or soaked in solutions of alcohol guests displayed absorption of the alcohols with repeatable stoichiometry affording well-ordered host−guest complexes.[48] Given that each macrocyclic unit has two oxygens with unsatisfied lone pairs, it is reasonable that guests with single hydrogen bond donors, such as TFE, phenol, and pentafluorophenol, were bound in 1:2 host/guest ratio. In contrast, ethylene glycol, which presents two hydrogen bond donors, was bound in a 1:1 ratio. The strong pillars of self-assembled **3** can simply move further apart, much like clays, to allow the reversible uptake of guests with a large range of shapes and sizes. The organization and spatial arrangement of the guests are controlled through the noncovalent intermolecular interactions. Pentafluoroiodobenzene and iodine were also absorbed by assembled **3**. A crystal structure of the pentafluoroiodobenzene cocrystallized with a urea protected derivative of macrocycle **3** showed surprisingly short halogen bonds between the iodo and the urea oxygen with I···O distances of 2.719 and 2.745 Å suggesting a strong interaction.[49] Thus, both hydrogen and halogen bonding can be used to drive solid-to-solid transformations of host **3**.

The dynamic expansion and contraction of the solid **3** during guest absorption and desorption provides a relatively flexible,

responsive binding site with fewer constraints compared with an interior channels of nanotubes. These two systems provide complementary strategies to organizing guests. Binding of guests and reactants into cavities, pores, channels, and crystals can restrict the motions of the reactants with respect to what occurs in solution. The restricted motion and preorganization of reactants can give rise to selectivity and even direct the formation of products that are not observed in solution. Next, we will focus on the structure of the channels within the bis-urea macrocycle assembly, address the binding of guests and reactants, and finally investigate the reactivity of these guests in confinement.

Bis-urea macrocycles that contain sizable cavities afford molecular crystals with aligned and homogeneous one-dimensional channels. The solvent that fills the channels can be highly ordered, as observed for AcOH in host 6,[31] or quite disordered, as seen for DMSO in host 7 or nitrobenzene in host 2.[32,21] These one-dimensional channels are of interest due to their simple shape and high uniformity, much like carbon nanotubes[50] and peptide nanotubes.[51] Figure 8 illustrates the packing of smaller benzophenone 7 nanotubes, which have an accessible channel of <6.5 Å in diameter, and the larger phenylethynylene 2 nanotubes, which have a channel diameter of ~9 Å. The view along the crystallographic b axis highlights

the density of aligned microchannels that are created in these molecular crystals. The guests in these crystals were omitted for clarity.

Heating removes the crystallization solvent leaving behind guest accessible channels and forming porous crystals that are stable up to 250 °C.[30] This process can be followed using thermogravimetric analysis (TGA), and the "empty" hosts show type 1 gas adsorption isotherms with $CO_2(g)$, which are indicative of microporous materials. Hosts 2, 6, and 7 display surface areas of 349,[21] 316,[30] and 320 m^2/g, respectively,[32] which are comparable to zeolites such as CxZSM-5,[52] albeit much smaller than the surface areas of porous molecular crystals and MOFs.

The gas adsorption data suggests that each of these hosts retains accessible microchannels; however, to further investigate the structures of these materials, we turned to powder X-ray diffraction. The single crystal data for hosts 2, 6, and 7 was used to generate a theoretical PXRD pattern for each system. Comparison of these patterns to those of the bulk crystals of hosts 2, 6, and 7 suggest that each is single phase and that the bulk crystals have similar structure to their corresponding single crystals. Heating removes the guests and in each case forms an empty host that is well ordered. Figure 9 compares the
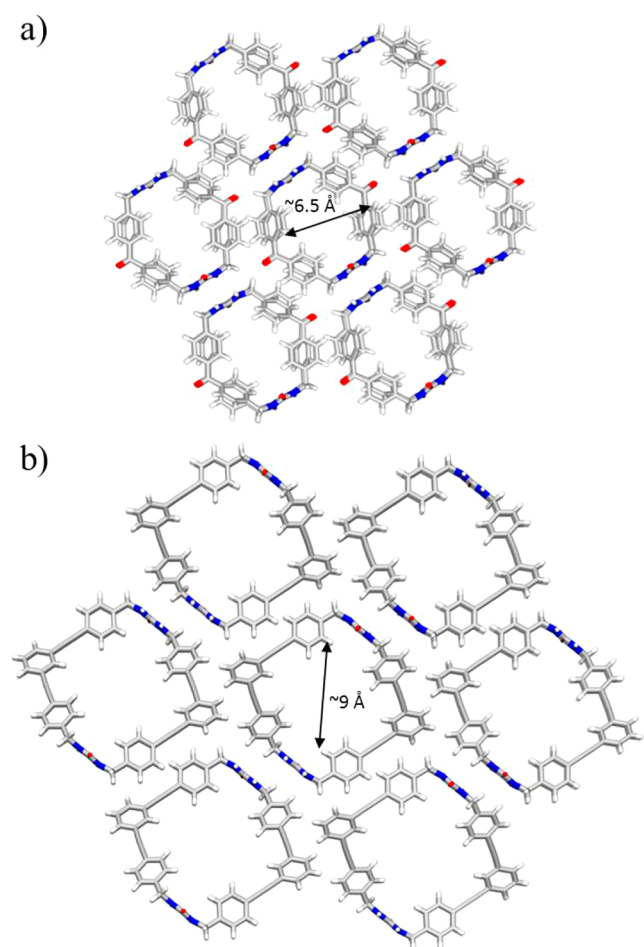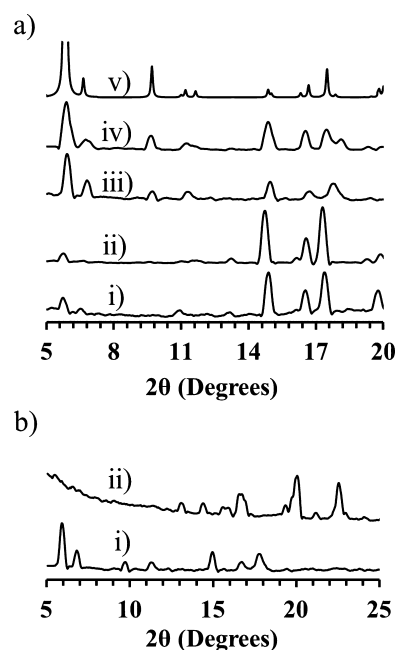

Figure 8. Columnar assembly and subsequent packing of the columns affords aligned one-dimensional channels. These are viewed down the b-axis of seven hydrogen-bonded tubes of the assembled (a) benzophenone macrocycles 7 (DMSO guests omitted)[32] and (b) phenylethynylene macrocycles 2 (nitrobenzene guests omitted).[21]

Figure 9. PXRD analysis of host 2 and its complexes.[21] (a) Comparison of the host 2 crystal forms and solvent free forms: (i) host 2·DMSO crystallized from DMSO; (ii) host 2·nitrobenzene crystallized from 2:8 DMSO/nitrobenzene; (iii) after heating host 2·DMSO to remove solvent; (iv) after heating host 2·nitrobenzene to remove solvent; (v) calculated pattern after removing the nitrobenzene guest. (b) PXRD pattern of host 2 solvent free (i) and after coumarin absorption (ii).

crystalline forms of host 2 with their empty forms. The sharp and intense peaks in the PXRD patterns for phenylethynylene host 2 crystals grown from either DMSO or 2:8 solution of DMSO/nitrobenzene (Figure 9a, patterns i and ii) are closely matched, indicating that they have similar highly ordered crystalline forms although they were prepared under different crystallization conditions.[21] The guests in each of these crystal forms (disordered DMSO or nitrobenzene) were removed by
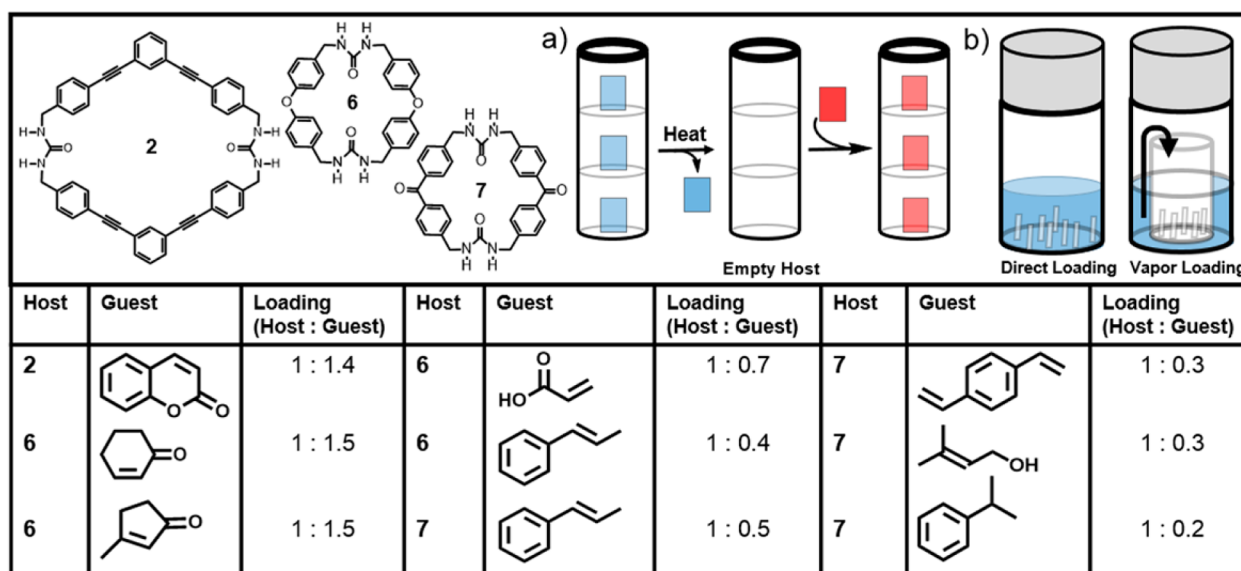
Figure 10. Absorption of guests by porous bis-urea hosts. (a) Schematic depiction of the desorption of solvent followed by exposure to a new guest to form a second host/guest complex. (b) Loading can be accomplished by soaking the empty host crystals in the neat liquid guest or in a solution that contains the guest or by exposing the host crystals to the guest vapor. The table shows examples of host/guest complexes formed by hosts **2**, **6**, and **7**.
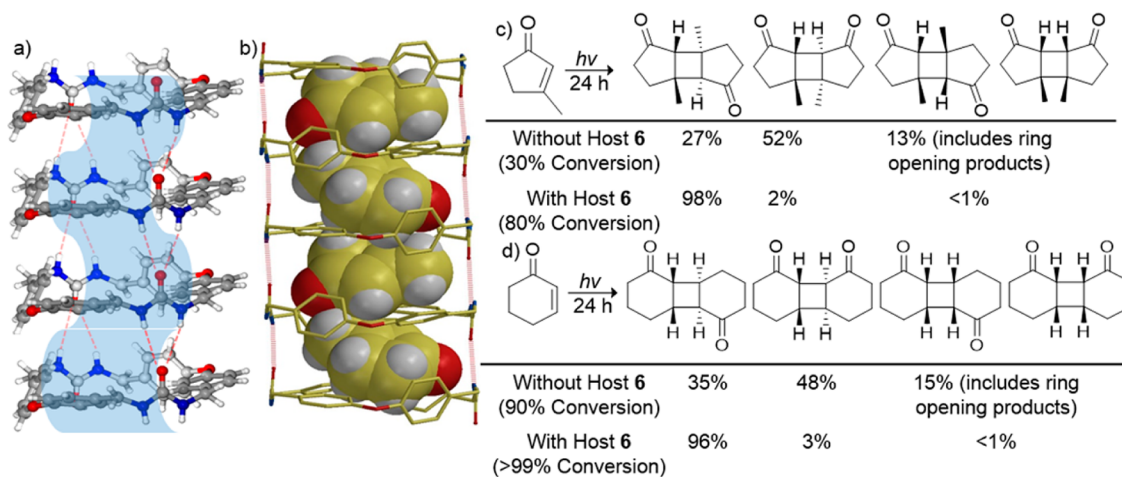

Figure 11. Host **6** facilitates [2 + 2] cycloaddition of enones.[56,57] (a) Schematic of the zigzag channel of the host. (b) Spartan models of 3-methyl-2-cyclopentene loaded in host **6** illustrate the guests bound head to tail. (c) UV irradiation of the host **6**·3-methyl-2-cyclopentene complex affords the *exo*-HT dimer in high conversion and selectivity. (d) UV irradiation of the host **6**·2-cyclohexene complex selectively affords the *exo*-HT dimer.

heating to generate the solvent free hosts (patterns iii and iv), which also have similar sharp, closely matched peaks, suggesting that they too have similar highly ordered structures. These patterns (iii and iv) are in good agreement with the simulated pattern of the empty host generated from the single crystal structure of **2**·nitrobenzene with the coordinates for the guest omitted (pattern v). Taken together the PXRD and gas adsorption suggest that the solvent-free structures have open channels that are similar in structure to the solvent filled columns.

Absorption of Guests within Columnar Nanotubes

Once the crystallization solvent has been removed by heating, a new guest can be loaded into the host (Figure 10a). Freshly obtained crystals of host **2** (15 mg) were heated from 25 to 170 °C (4 °C/min) to remove the DMSO solvent in the host **2** channels. Next, a new guest can then be introduced by several methods (Figure 10b) including (a) vapor loading, (b) soaking

directly in liquid guests, or (c) soaking in guest solutions (0.1–1.0 mM in a solvent that has low affinity for the channel). Cyclohexanone was readily loaded by exposing macrocycles **6** or **7** to its vapor in a sealed chamber (method a). For method b, crystals of macrocycle **2** (5–50 mg) were soaked in pure liquid (1 mL) in a scintillation vial. Alternatively, freshly evacuated crystals of host **2** were cooled under helium(g) and immersed in solutions of coumarin (0.1 mM in CH$_3$CN, method c). Guest absorption is monitored by thermogravimetric analysis (TGA), by ^{1}H NMR, or, when the guest contains a chromophore, by following the depletion of the guest from solution using absorption spectroscopy. The newly formed host−guest complexes were characterized in the solid-state using ^{13}C{^{1}H}CP-MAS NMR, powder X-ray diffraction (PXRD), and IR.

Hosts **2**, **6**, and **7** show a strong binding preference for polar guests, and no binding was observed for alkanes or cycloalkanes

even upon soaking in the neat liquid guests for 18–24 h. Hosts **6** and **7** have similar size channels, although the arrangement of their aryl groups affords slightly different shapes: zigzag (**6**) versus relatively straight (**7**). They bind a series of small organic guests including acrylic acid, THF, EtOAc, DMSO, and AcOH in similar ratios.[32] In general, small polar guests including enones were absorbed in higher ratios into the narrow channels of hosts **6** and **7**.[31,32] Branched alcohols, such as 3-methyl-2-buten-1-ol, and larger guests (styrene and divinylbenzene) formed complexes with lower host–guest ratios, consistent with the guests binding into a confined space. The phenylethynylene host **2** was able to form complexes with much larger coumarin and acenaphthalene guests.[21] These host–guest complexes typically display distinct, sharp, and intense peaks consistent with a well ordered structure. See Figure 9b for a comparison of the host **2** with its host **2**·coumarin complex.

When the reaction vessel is commensurate to the size of the reactants, it can dramatically influence the reaction process.[3] Molecular size cavities of porous materials have been used to modulate reactions and influence selectivity in solution and to template reactions in the solid state.[53] MacGillivray employs resorcinol templates with great success to organize olefin reactants in cocrystals and to direct the solid-state synthesis of complex ladderanes, a task difficult to achieve in solution.[54] Similarly, the nanochannels of crystalline assembled bis-ureas can be used to facilitate the reaction of encapsulated guests and to study the effects of the changes in the columnar framework on the reactions that occur inside.

Host **6** was used as a container to facilitate [2 + 2] photoreactions of enones in the solid state. The [2 + 2] cycloaddition has been applied to a number of natural products and pharmaceuticals,[55] and better control over the efficiency and selectivity of this reaction would further enhance its utility. The channel of host **6** is not straight, due to the orientation of the phenyl rings and their edge to face aryl stacking (Figure 11a). Enones including acrylic acid, methylvinylketone (MVK), 2-cyclohexenone, 2-methyl-2-cyclopentenone, and 3-methyl-2-cyclopentenone were readily loaded into host **6** to afford host–guest complexes.[56] UV irradiation of these solid complexes facilitated the [2 + 2] cyclodimerization in high conversion and selectivity for enones that matched the size and shape of the channel, while small substrates such as MVK did not react. Figure 11 illustrates some of these photodimerizations. For 3-methyl-2-cyclopentenone (Figure 11c), we observed high conversion (80%) and selectivity (98%) for the *exo* head-to-tail (HT) dimer in the presence of host **6**.[56] In contrast, the control shows low conversion (31%) and poor selectivity. Other enones including cyclohexanone also showed excellent conversion (>99%) and selectivity (96%) again for its corresponding *exo*-HT dimer.[57] Modeling studies with Spartan[58] suggest that these guests load into the zigzag channel in an alternating fashion (Figure 11b), where they are preorganized in close proximity and in favorable suprafacial geometries for selective reactions to their corresponding *exo*-HT dimers.

Small changes in the macrocycle framework (an ether in **6** to a carbonyl in **7**) did not affect the self-assembly or alter the channel size but predictably influenced the reactions that were favored in their respective nanochannels.[32] Host **7** contains the triplet sensitizer benzophenone, while host **6** lacks a sensitizer. Literature suggests that enone photodimerization is unfavorable in the presence of triplet sensitizers.[59] Ten enones tested, including those that underwent selective photocycloaddition

reactions within host **6**, were found to be unreactive within host **7** even after prolonged UV irradiation.[32,60] In contrast, reactions that require a sensitizer were facilitated by host **7** but did not occur with host **6**. For example, host **7** induced a rapid *cis–trans* isomerization of *trans-β*-methyl-styrene, a reaction that was not observed in the presence of **6**.[32]

The photophysical properties of benzophenone may be modulated by the macrocyclic framework, as well as by the subsequent supramolecular assembly due to the proximity of other groups. We observed modest differences in the photophysical properties between benzophenone and unassembled host **7** in solution. In contrast, upon assembly there was a dramatic shortening of benzophenone's phosphorescent lifetime from 22.6 μs for benzophenone to <1 ns for assembled **7**, as well as the formation of a stable radical species.[61] Despite the reduced lifetime of the excited state, UV-irradiation of **7** suspended in an oxygenated solution of chloroform efficiently produced singlet oxygen, which was identified by its characteristic emission in the near IR (Figure 12a,b).
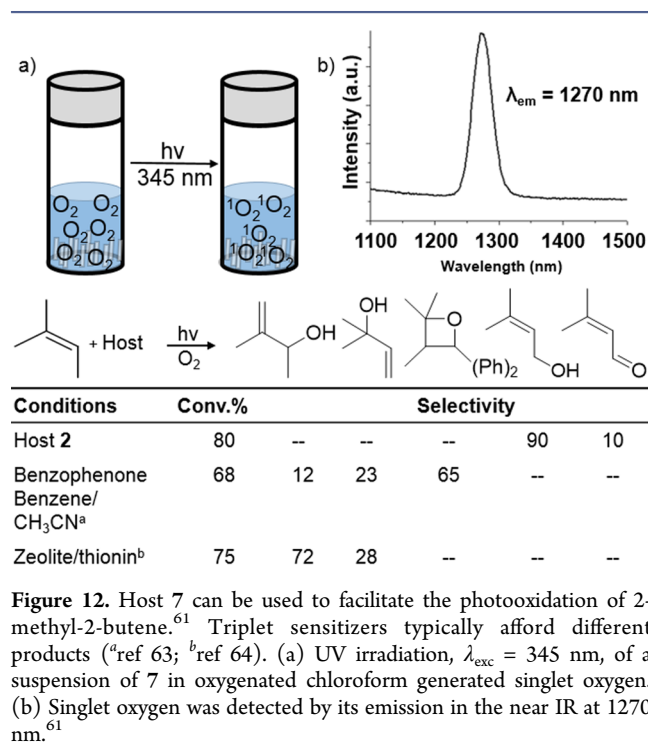

Conditions	Conv.%			Selectivity		
Host **2**	80	--	--	--	90	10
Benzophenone Benzene/ CH_3CN^a	68	12	23	65	--	--
Zeolite/thionin[b]	75	72	28	--	--	--

Figure 12. Host **7** can be used to facilitate the photooxidation of 2-methyl-2-butene.[61] Triplet sensitizers typically afford different products (*a*ref 63; *b*ref 64). (a) UV irradiation, λ_{exc} = 345 nm, of a suspension of **7** in oxygenated chloroform generated singlet oxygen. (b) Singlet oxygen was detected by its emission in the near IR at 1270 nm.[61]

Singlet oxygen, an atom economic oxidant, is very reactive, is difficult to control, and often affords a mixture of products. Host **7** facilitated a selective oxidation of bound 2-methyl-2-butene to afford 3-methyl-2-butene-1-ol (80% conversion at 2 h).[61] This allylic alcohol is not observed in solution with benzophenone or with other sensitizers.[62−64] UV irradiation of host **7**·cumene afforded the tertiary alcohol, α,α′-dimethyl benzyl alcohol, at 64% selectivity, an observation that suggests that these oxidation reactions may proceed through radical pathways. We are currently studying this mechanism and hope to extend this work to heterogeneous processes, where the solid host might be used as a catalyst in solution.

The wider channels of phenylethynylene host **2** (diameter of ∼9 Å) can accommodate much larger guests including coumarin to form stable host–guest complexes. Figure 9b, spectrum ii, shows that the PXRD pattern is sharp, indicative of a highly ordered material, and distinct from the empty host.[21]

In the solid state, the photodimerization of coumarin is a reversible reaction and proceeds in low conversion (<5%) to four photodimers (Figure 13).[65] In solution, Ramamurthy's

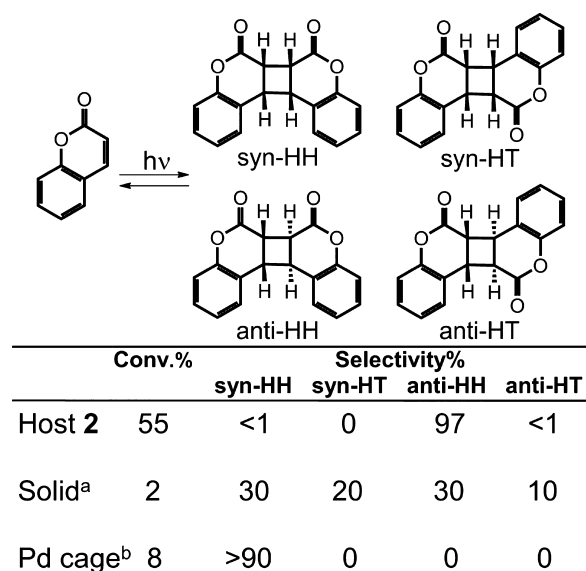|	Conv.%	Selectivity%			
		syn-HH	syn-HT	anti-HH	anti-HT
Host **2**	55	<1	0	97	<1
Solid[a]	2	30	20	30	10
Pd cage[b]	8	>90	0	0	0

Figure 13. The photolysis of coumarin affords four possible dimers. Conversion is limited in the solid state ([a]ref 65). Hosts, such as Fujita's Pd nanocage ([b]ref 66) and bis-urea host **2**,[21] have been used to tune the selectivity of the photodimerization.

group demonstrated that confinement using a Pd nanocage in D_2O afforded high selectivity (90%) for the *syn*-head-to-head (HH) dimer.[66] In comparison, UV irradiation of the solid host **2**·coumarin complex under Ar(g) afforded the *anti*-HH photodimer of the coumarin in 97% selectivity.[21] Subjecting host **2**·coumarin to longer reaction times increased the conversion up to 55%, suggesting that the confinement with host **2** may be slowing the reverse reaction or stabilizing the photodimer. This conversion limit may be a result of inefficient light penetration, multiple guest binding sites, or other factors.

SUMMARY AND FUTURE PERSPECTIVES

Bis-urea macrocycles have proven to be versatile building blocks for constructing pillars and columnar nanotubes. Our work on the pyridyl derivatives suggests that one not only should heed the supramolecular interactions that result in strong one-dimensional pillars but also should consider how these structures further assemble. Indeed, providing a guest that could satisfy accessible basic urea oxygen lone pairs on the exterior of these pillars was enough to allow these pillared solids to expand through a solid-to-solid process and effectively order the guests in layers between the pillars. It remains to be seen whether such a strategy could be applied broadly to organize alcohol and electrophilic halide derivatives in the solid state. Control of the spatial arrangement and organization of chromophores is of particular importance for sensing and in molecular electronics.

Macrocyclic bis-ureas with interior channels assembled in high fidelity to afford porous crystals with homogeneous channels. Single crystal X-ray analysis provides beautiful maps of these channels, which have dimensions set by the macrocycle and are typically filled with the crystallization solvent. Removal of the solvent by heating affords a solid host with homogeneous channels that have high absorption capacity for guests that

match the channels' size, shape, and polarity. This control over topology, shape, and functionality of a simple one-dimensional channel is advantageous for investigating fundamental questions of diffusion, molecular transport, and reactivity in confinement. Our group is actively exploring reactions within these tiny spaces with respect to their mechanisms, conversion rates, and potential applications in catalysis. Collaborations with C. Russ Bowers and Sergey Vasenkov (UFl) are probing molecular transport processes by pulsed field gradient NMR and hyperpolarized Xenon-129 tracer exchange NMR. We hope to share our findings on these issues in the near future.

AUTHOR INFORMATION

Corresponding Author

*E-mail: shimizls@mailbox.sc.edu.

Notes

The authors declare no competing financial interest.

Biographies

Linda Shimizu received her B.A. from Wellesley College and her Ph.D. from the Massachusetts Institute of Technology (MIT) in 1997 under the guidance of Prof. Daniel Kemp. She was a NIH postdoctoral fellow with Prof. John Essigmann also at MIT. She joined the University of South Carolina and was promoted to Associate Professor with tenure in 2011. Professor Shimizu received an American Chemical Society Women Chemists Committee Rising Star 2013 Award and was named a 2011 Breakthrough Rising Star by the University of South Carolina Office of Research. She is a member of the Advisory Board for the Inter-American Photochemical Society (IAPS) and was a Co-organizer of the 23rd Winter I-APS meeting January 2014. Her research interests include organic photochemistry, supramolecular assembly, materials chemistry, and crystal engineering.

Sahan Salpage received his B.Sc. (chemistry) with Honors from the Institute of Chemistry, College of Chemical Sciences, Sri Lanka, in 2008. He then moved to the University of South Carolina in 2011 to work on his Ph.D. with Prof. Shimizu.

Arthur Korous received his bachelors in science from Winthrop University, College of Arts and Sciences, in 2013. He is currently pursuing his Ph.D. at the University of South Carolina under the guidance of Prof. Shimizu.

REFERENCES

(1) Wu, H. H.; Gong, Q. H.; Olson, D. H.; Li, J. Commensurate adsorption of hydrocarbons and alcohols in microporous metal organic frameworks. *Chem. Rev.* **2012**, *112*, 836−868.

(2) Bae, Y. S.; Snurr, R. Q. Development and evaluation of porous materials for carbon dioxide separation and capture. *Angew. Chem., Int. Ed.* **2011**, *50*, 11586−11596.

(3) Inokuma, Y.; Kawano, M.; Fujita, M. Crystalline molecular flasks. *Nat. Chem.* **2011**, *3*, 349−358.

(4) Bocquet, L.; Charlaix, E. Nanofluidics, from bulk to interfaces. *Chem. Soc. Rev.* **2010**, *39*, 1073−1095.

2125

dx.doi.org/10.1021/ar500106f | *Acc. Chem. Res.* 2014, 47, 2116−2127

(5) Perego, C.; Millini, R. Porous materials in catalysis: Challenges for mesoporous materials. *Chem. Soc. Rev.* **2013**, *42*, 3956−3976.

(6) Sumida, K.; Rogow, D. L.; Mason, J. A.; McDonald, T. M.; Bloch, E. D.; Herm, Z. R.; Bae, T.-H.; Long, J. R. Carbon dioxide capture in metal−organic frameworks. *Chem. Rev.* **2012**, *112*, 724−781.

(7) Tao, Y. S.; Kanoh, H.; Abrams, L.; Kaneko, K. Mesopore-modified zeolite: Preparation, characterization and applications. *Chem. Rev.* **2006**, *106*, 896−910.

(8) Ruiz-Hitzky, E.; Aranda, P.; Belver, C. Nanoarchitectures based on clay materials. In *Manipulation of Nanoscale Materials*; Ariga, K., Ed.; RSC Nanoscience & Nanotechnology Series; RSC Publishing: Cambridge, U.K., 2012; Vol. 24, pp 87−111.

(9) Vinu, A.; Hossain, K. Z.; Ariga, K. Recent advances in functionalization of mesoporous silica. *J. Nanosci. Nanotechnol.* **2005**, *5*, 347−371.

(10) Magner, E. Immobilisation of enzymes on mesoporous silicate materials. *Chem. Soc. Rev.* **2013**, *42*, 6213−6222.

(11) Mastalerz, M. Permanent porous materials from discrete organic molecules − Towards ultra-high surface areas. *Chem.—Eur. J.* **2012**, *18*, 10082−10091.

(12) Tranchemontagne, D. J.; Mendoza-Cortes, J. L.; O'Keeffe, M.; Yaghi, O. M. Secondary building units, nets and bonding in the chemistry of metal-organic frameworks. *Chem. Soc. Rev.* **2009**, *38*, 1257−1283.

(13) Busseron, E.; Ruff, Y.; Moulin, E.; Giuseppone, N. Supra-molecular self-assemblies as functional nanomaterials. *Nanoscale* **2013**, *5*, 7098−7140.

(14) Ghadiri, M. R.; Granja, J. R.; Milligan, R. A.; McRee, D. E.; Khazanovich, N. Self-assembling organic nanotubes based on a cyclic peptide architecture. *Nature* **1993**, *366*, 324−327.

(15) Bong, D. T.; Clark, T. D.; Granja, J. R.; Ghadiri, M. R. Self-assembling organic nanotubes. *Angew. Chem., Int. Ed.* **2001**, *40*, 988−1011.

(16) Zang, L.; Che, Y.; Moore, J. S. One-dimensional self-assembly of planar π-conjugated molecules: Adaptable building blocks for organic nanodevices. *Acc. Chem. Res.* **2008**, *41*, 1596−1608.

(17) Frischmann, P. D.; Sahli, B. J.; Guieu, S.; Patrick, B. O.; MacLachlan, M. J. Sterically-limited self-assembly of Pt4 macrocycles into discrete non-covalent nanotubes: Porous supramolecular tetramers and hexamers. *Chem.—Eur. J.* **2012**, *18*, 13712−13721.

(18) Gong, B.; Shao, Z. Self-assembling organic nanotubes with precisely defined, sub-nanometers pores: Formation and mass transport characteristics. *Acc. Chem. Res.* **2013**, *46*, 2856−2866.

(19) McKeown, N. B. Nanoporous molecular crystals. *J. Mater. Chem.* **2010**, *20*, 10588−10597.

(20) Shimizu, L. S.; Smith, M. D.; Hughes, A. D.; Shimizu, K. D. Self-assembly of a bis-urea macrocycle into a columnar nanotube. *Chem. Commun.* **2001**, 1592−1593.

(21) Dawn, S.; Dewal, M. B.; Sobransingh, D.; Paderes, M. C.; Wibowo, A. C.; Smith, M. D.; Krause, J. A.; Pellechia, P. J.; Shimizu, L. S. Porous crystals from self-assembled phenylethynylene bis-urea macrocycles facilitate the selective photodimerization of coumarin. *J. Am. Chem. Soc.* **2011**, *133*, 7025−7032.

(22) Burada, P. S.; Hanggi, P.; Marchesoni, F.; Schmid, G.; Talkner, P. Diffusion in confined geometries. *ChemPhysChem* **2009**, *10*, 45−54.

(23) Roy, K.; Wang, C.; Smith, M. D.; Dewal, M. B.; Wibowo, A. C.; Brown, J. C.; Ma, S.; Shimizu, L. S. Guest induced transformations of assembled pyridyl bis-urea macrocycles. *Chem. Commun.* **2011**, *47*, 277−279.

(24) Hunter, C. A. Quantifying intermolecular interactions: Guidelines for the molecular recognition toolbox. *Angew. Chem., Int. Ed.* **2004**, *43*, 5310−5324.

(25) Etter, M. C.; Urbanczyk-Lipkowska, Z.; Zia-Ebrahimi, M.; Panunto, T. W. Hydrogen bond directed cocrystallization and molecular recognition properties of diarylureas. *J. Am. Chem. Soc.* **1990**, *112*, 8415−8426.

(26) Steed, J. W. Anion tuned supramolecular gels: a natural evolution from urea supramolecular chemistry. *Chem. Soc. Rev.* **2010**, *39*, 3686−3699.

(27) Custelcean, R. Crystal engineering with urea and thiourea hydrogen-bonding groups. *Chem. Commun.* **2008**, 295−307.

(28) Petersen, H. Syntheses of cyclic ureas by alpha-ureidoalkylation. *Synthesis* **1973**, 243−292.

(29) Yang, J.; Dewal, M. B.; Sobransingh, D.; Smith, M. D.; Xu, Y.; Shimizu, L. S. Examination of the structural features that favor the columnar self-assembly of bis-urea macrocycles. *J. Org. Chem.* **2009**, *74*, 102−110.

(30) Dewal, M. B.; Lufaso, M. W.; Hughes, A. D.; Samuel, S. A.; Pellechia, P.; Shimizu, L. S. Absorption properties of a porous organic crystalline apohost formed by a self-assembled bis-urea macrocycle. *Chem. Mater.* **2006**, *18*, 4855−4864.

(31) Shimizu, L. S.; Hughes, A. D.; Smith, M. D.; Davis, M. J.; Zhang, P.; zur Loye, H.-C.; Shimizu, K. D. Self-assembly of a bis-urea macrocycle into a columnar nanotube. *J. Am. Chem. Soc.* **2003**, *125*, 14972−14973.

(32) Dewal, M. B.; Xu, Y.; Yang, J.; Mohammed, F.; Smith, M. D.; Shimizu, L. S. Manipulating the cavity of a porous material changes the photoreactivity of included guests. *Chem. Commun.* **2008**, 3909−3911.

(33) Macrae, C. F.; Edgington, P. R.; McCabe, P.; Pidcock, E.; Shields, G. P.; Taylor, R.; Towler, M.; van de Streek, J. Mercury: Visualization and analysis of crystal structures. *J. Appl. Crystallogr.* **2006**, *39*, 453−457.

(34) Xu, Y.; Xu, W. L.; Smith, M. D.; Shimizu, L. S. Self-assembly and ring opening metathesis polymerization of bifunctional carbonate-stilbene macrocycles. *RSC Adv.* **2014**, *4*, 1675−1682.

(35) Feng, J.; Zhuo, R.-X.; Zheng, X. Z. Construction of functional aliphatic polycarbonates for biomedical applications. *Prog. Polym. Sci.* **2012**, *37*, 211−236.

(36) Roy, K.; Wang, C.; Smith, M. D.; Pellechia, P. J.; Shimizu, L. S. Alkali metal ions as probes of structure and recognition properties of macrocyclic pyridyl urea hosts. *J. Org. Chem.* **2010**, *75*, 5453−5460.

(37) Roy, K.; Smith, M. D.; Shimizu, L. S. 1D coordination network formed by a cadmium based pyridyl urea helical monomer. *Inorg. Chim. Acta* **2011**, *376*, 598−604.

(38) Shimizu, L. S.; Smith, M. D.; Hughes, A. D.; Samuel, S.; Ciurtin-Smith, D. Assembled tubular structures from bis-urea macrocycles. *Supramol. Chem.* **2005**, *17*, 27−30.

(39) Geer, M. F.; Smith, M. D.; Shimizu, L. S. A bis-urea naphthalene macrocycle displaying two crystal structures with parallel ureas. *CrystEngComm* **2011**, *13*, 3665−3669.

(40) Tian, L.; Wang, C.; Dawn, S.; Smith, M. D.; Krause, J. A.; Shimizu, L. S. Macrocycles with switchable *exo/endo* metal binding sites. *J. Am. Chem. Soc.* **2009**, *131*, 17620−17629.

(41) Henze, O.; Lentz, D.; Schäfer, A.; Franke, P.; Schlüter, A. D. Phenylacetylene macrocycles with two opposing bipyridine donor sites: Syntheses, X-ray structure determinations, and Ru complexation. *Chem.—Eur. J.* **2002**, *8*, 357−365.

(42) Irving, H.; Williams, R. J. P. The stability of transition-metal complexes. *J. Chem. Soc.* **1953**, 3192−3210.

(43) Dawn, S.; Salpage, S. R.; Smith, M. D.; Sharma, S. K.; Shimizu, L. S. A trinuclear silver coordination polymer from a bipyridine bis-urea macrocyclic ligand and silver triflate. *Inorg. Chem. Commun.* **2012**, *15*, 88−92.

(44) Naodovic, M.; Yamamoto, H. Asymmetric silver-catalyzed reactions. *Chem. Rev.* **2008**, *108*, 3132−3148.

(45) Prier, C. K.; Rankic, D. A.; MacMillan, D. W. C. Visible light photoredox catalysis with transition metal complexes: Applications in organic synthesis. *Chem. Rev.* **2013**, *113*, 5322−5363.

(46) Beer, P. D.; Gale, P. A. Anion recognition and sensing: The state of the art and future perspectives. *Angew. Chem., Int. Ed.* **2001**, *40*, 486−516.

(47) Murray, T. J.; Zimmerman, S. C. New triply hydrogen bonded complexes with highly variable stabilities. *J. Am. Chem. Soc.* **1992**, *114*, 4010−4011.

(48) Roy, K.; Wibowo, A. C.; Pellechia, P. J.; Ma, S.; Geer, M. F.; Shimizu, L. S. Absorption of hydrogen bond donors by pyridyl bis-urea crystals. *Chem. Mater.* **2012**, *24*, 4773−4781.

(49) Geer, M. F.; Mazzuca, J.; Smith, M. D.; Shimizu, L. S. Short strong halogen bonding in co-crystals of pyridyl bis-urea macrocycles and iodo perfluorocarbons. *CrystEngComm* **2013**, *15*, 9923−9929.

(50) Fornasiero, F.; Park, H. G.; Holt, J. K.; Stadermann, M.; Grigoropoulos, C. P.; Noy, A.; Bakajin, O. Ion exclusion by sub-2-nm carbon nanotube pores. *Proc. Natl. Acad. Sci. U. S. A.* **2008**, *105*, 17250−17255.

(51) Cheng, C.-Y.; Bowers, C. R. Direct observation of atoms entering and exiting L-Alanyl-L-valine nanotubes by hyperpolarized xenon-129 NMR. *J. Am. Chem. Soc.* **2007**, *129*, 13997−14002.

(52) Yamazaki, T.; Katoh, M.; Ozawa, S.; Ogino, Y. Adsorption of CO_2 over univalent cation-exchanged ZSM-5 zeolites. *Mol. Phys.* **1993**, *80*, 313−324.

(53) Ramamurthy, V.; Parthasarathy, A. Chemistry in restricted spaces: Select photodimerizations in cages, cavities, and capsules. *Isr. J. Chem.* **2011**, *51*, 817−829.

(54) MacGillivray, L. R.; Papaefstathiou, G. S.; Friščić, T.; Hamilton, T. D.; Bučar, D. K.; Chu, Q.; Varshney, D. B.; Georgiev, I. G. Supramolecular control of reactivity in the solid state: From templates to ladderanes to metal organic frameworks. *Acc. Chem. Res.* **2008**, *41*, 280−291.

(55) Iriondo-Alberdi, J.; Greaney, M. F. Photocycloaddition in natural product synthesis. *Eur. J. Org. Chem.* **2007**, 4801−4815.

(56) Yang, J.; Dewal, M. B.; Profeta, S.; Smith, M. D.; Li, Y.; Shimizu, L. S. Origins of selectivity for the [2 + 2] cycloaddition of α,β-unsaturated ketones within a porous self-assembled organic framework. *J. Am. Chem. Soc.* **2008**, *130*, 612−621.

(57) Yang, J.; Dewal, M. B.; Shimizu, L. S. Self-assembling bis-urea macrocycles used as an organic zeolite for a highly stereoselective photodimerization of 2-cyclohexenone. *J. Am. Chem. Soc.* **2006**, *128*, 8122−8123.

(58) Spartan 04 for Macintosh, v. 1.1.1, 2007, Wavefunction, Inc., Irvine, CA.

(59) De Mayo, P.; Pete, J.-P.; Tchir, M. Cyclopentenone photocycloaddition. A reaction from a higher triplet State. *J. Am. Chem. Soc.* **1967**, *89*, 5712−5713.

(60) Dewal, M. B. Design, Synthesis, and Applications of Porous Crystals from Self-Assembled Bis-Urea Macrocycles. Ph.D. Dissertation, University of South Carolina, Columbia, SC, 2008.

(61) Geer, M. F.; Walla, M. D.; Solntsev, K. M.; Strassert, C. A.; Shimizu, L. S. Self-assembled benzophenone bis-urea macrocycles facilitate selective oxidations by singlet oxygen. *J. Org. Chem.* **2013**, *78*, 5568−5578.

(62) Foote, C. S. Photosensitized oxygenations and the role of singlet oxygen. *Acc. Chem. Res.* **1968**, *1*, 104−110.

(63) Shimizu, N.; Bartlett, P. D. Photooxidation of olefins sensitized by α-diketones and by benzophenone. A practical epoxidation method with biacetyl. *J. Am. Chem. Soc.* **1976**, *98*, 4193−4200.

(64) Robbins, R. J.; Ramamurthy, V. Generation and reactivity of singlet oxygen within zeolites: Remarkable control of hydroperoxidation of alkenes. *Chem. Commun.* **1997**, 1071−1072.

(65) Tanaka, K.; Toda, F. Solvent free organic synthesis. *Chem. Rev.* **2000**, *100*, 1025−1074.

(66) Karthikeyan, S.; Ramamurthy, V. Templating photodimerization of coumarins within a water soluble nano reation vessel. *J. Org. Chem.* **2006**, *71*, 6409−6413.